climate

MDPI

Article

Rising Precipitation Extremes across Nepal

Ramchandra Karki [1,2,*], Shabeh ul Hasson [1,3], Udo Schickhoff [1], Thomas Scholten [4] and Jürgen Böhner [1]

1 Center for Earth System Research and Sustainability, Institute of Geography, University of Hamburg, Bundesstraße 55, 20146 Hamburg, Germany; shabeh.hasson@uni-hamburg.de (S.H.); udo.schickhoff@uni-hamburg.de (U.S.); juergen.boehner@uni-hamburg.de (J.B.)
2 Department of Hydrology and Meteorology, Government of Nepal, 406 Naxal, Kathmandu, Nepal
3 Department of Space Sciences, Institute of Space Technology, Islamabad 44000, Pakistan
4 Soil Science and Geomorphology, University of Tübingen, Department of Geosciences, Rümelinstrasse 19-23, 72070 Tübingen, Germany; thomas.scholten@uni-tuebingen.de
* Correspondence: Ramchandra.Karki@studium.uni-hamburg.de; Tel.: +49-40-428-383-826

Academic Editor: Christina Anagnostopoulou
Received: 10 November 2016; Accepted: 6 January 2017; Published: 13 January 2017

Abstract: As a mountainous country, Nepal is most susceptible to precipitation extremes and related hazards, including severe floods, landslides and droughts that cause huge losses of life and property, impact the Himalayan environment, and hinder the socioeconomic development of the country. Given that the countrywide assessment of such extremes is still lacking, we present a comprehensive picture of prevailing precipitation extremes observed across Nepal. First, we present the spatial distribution of daily extreme precipitation indices as defined by the Expert Team on Climate Change Detection, Monitoring and Indices (ETCCDMI) from 210 stations over the period of 1981–2010. Then, we analyze the temporal changes in the computed extremes from 76 stations, featuring long-term continuous records for the period of 1970–2012, by applying a non-parametric Mann−Kendall test to identify the existence of a trend and Sen's slope method to calculate the true magnitude of this trend. Further, the local trends in precipitation extremes have been tested for their field significance over the distinct physio-geographical regions of Nepal, such as the lowlands, middle mountains and hills and high mountains in the west (WL, WM and WH, respectively), and likewise, in central (CL, CM and CH) and eastern (EL, EM and EH) Nepal. Our results suggest that the spatial patterns of high-intensity precipitation extremes are quite different to that of annual or monsoonal precipitation. Lowlands (Terai and Siwaliks) that feature relatively low precipitation and less wet days (rainy days) are exposed to high-intensity precipitation extremes. Our trend analysis suggests that the pre-monsoonal precipitation is significantly increasing over the lowlands and CH, while monsoonal precipitation is increasing in WM and CH and decreasing in CM, CL and EL. On the other hand, post-monsoonal precipitation is significantly decreasing across all of Nepal while winter precipitation is decreasing only over the WM region. Both high-intensity precipitation extremes and annual precipitation trends feature east−west contrast, suggesting significant increase over the WM and CH region but decrease over the EM and CM regions. Further, a significant positive trend in the number of consecutive dry days but significant negative trend in the number of wet (rainy) days are observed over the whole of Nepal, implying the prolongation of the dry spell across the country. Overall, the intensification of different precipitation indices over distinct parts of the country indicates region-specific risks of floods, landslides and droughts. The presented findings, in combination with population and environmental pressures, can support in devising the adequate region-specific adaptation strategies for different sectors and in improving the livelihood of the rural communities in Nepal.

Keywords: Nepal; spatial precipitation pattern; precipitation extremes; consecutive dry days; high-intensity precipitation

1. Introduction

Precipitation extremes are one of the major factors that trigger natural disasters, such as droughts, floods and landslides, which subsequently cause the loss of property and life, and deteriorate socioeconomic development. Under the prevailing anthropogenic warming, the precipitation extremes are observed to be intensified globally, exacerbating the existing problems of food and water security as well as disaster management [1–11].

Consistent with the global pattern [4,10], the world's most disaster-prone region of South Asia [12] has also experienced an overall increase in precipitation extremes [11], though such a pattern is heterogeneous across the region [5,11,13,14]. For instance, studies have found a rise in the summer monsoonal precipitation extremes over central India and northeastern Pakistan [15–20]. In contrast, precipitation extremes feature a falling trend over southwestern Pakistan [20], the eastern Gangetic plains and some parts of Uttaranchal, India [21]. Further, contrary to the extremes observed at low altitudes or over the plains, extremes observed in the high-altitude mountainous regions exhibit quite an opposite sign of change due to the influence of local factors, and are thus less predictable [22].

Situated in the steep terrain of the central Himalayan range, Nepal is likewise more susceptible to the developments of heavy rainfall events and subsequent flooding and droughts severely impacting the marginalized mountain communities, as was impressively illustrated by recent events. For instance, the cloudburst of 14–17 June 2013 in the northwestern mountainous region near the Nepalese border killed around 5700 people and affected more than 100,000, extensively damaging the property in both Nepal and India [23]. A heavy rain event of 14–16 August 2014 likewise caused massive flooding and triggered a number of landslides, resulting in huge losses of life and property, affecting around 35,000 households [24]. Similarly, one of the worst winter droughts of the country in 2008/2009 reduced yield of wheat and barley by 14% and 17%, respectively, leading to severe food shortage in 66% of rural households in the worst hit far- and mid-western hill and mountain regions [25]. Such intense precipitation and extreme dryness (droughts) negatively impact the yield of both cash and cereal crops [26], and in turn, the livelihood of around 60% of the total Nepalese population directly dependent on agriculture [27]. Therefore, analyzing the precipitation extremes and their time evolution under prevailing climatic changes is of paramount importance for ensuring food and water security in Nepal and developing a region-specific disaster management strategy.

As compared to the rest of South Asia, studies on the observed precipitation extremes over Nepal are rare and sporadic, lacking a comprehensive picture across the country. For instance, computing various extreme precipitation indices from only 26 stations for the period of 1961–2006, Baidya et al. [28] have found an increasing trend in total events and heavy precipitation events from most of the stations. In contrast, analyzing only a subset of extreme precipitation indices used in Baidya et al. [28], from the daily interpolated gridded precipitation of APHRODITE (1951–2007) Duncan et al. [29] concludes that the monsoonal and annual precipitation extremes are unlikely to worsen over Nepal. Since precipitation extremes are more localized and can be smoothed over when limited gauge data is interpolated [30], employing APHRODITE may have significantly affected the computation of extreme statistics as it hardly incorporates any real observations from the early 1950s west of Kathmandu [31]. Recently, analyzing the extreme precipitation indices only within the Koshi River basin in eastern Nepal for the 1975–2010 period, Shrestha et al. [32] have reported an overall increase in the precipitation total and intensity, though such trends were statistically insignificant. These discordant findings of changes in the precipitation extremes over Nepal may be attributed to employing varying datasets, analyzing different time periods, and focusing on distinct study regions, hence lacking a countrywide picture.

In view of these limited countrywide studies with contrasting findings—and because an understanding of the extreme precipitation events is crucial to socioeconomic development—, this study presents an exploratory analysis of the widely adopted daily precipitation extremes across the whole of Nepal based on the maximum number of high-quality long-term station observations. For this, the extreme indices from the Expert Team on Climate Change Detection, Monitoring and

Indices (ETCCDMI) along with a few additional indices are computed from the daily precipitation observations. First, we have analyzed the spatial distribution of the most relevant precipitation extremes as well as the seasonal precipitation patterns from 210 surface weather stations across Nepal over the most recent period, 1981–2010. Moreover, time evolution of the computed precipitation extremes has been analyzed by ascertaining the monotonic trends from the long-term continuous record available at 76 stations over the 1970–2012 period. In this regard, a robust non-parametric Mann−Kendall [33,34] trend test along with the trend free pre-whitening (TFPW) procedure has been applied. The trends at the local stations are further assessed for their field significance over the distinct physio-geographic regions of Nepal, in order to establish the dominant patterns of changes in precipitation extremes.

2. Study Area

Nepal is a mountainous country that stretches between 26.36° N–30.45° N and 80.06° E–88.2° E, encompassing an area of 147,181 km^2 and an elevation range of 60–8848 m above sea level (asl). Along the cardinal directions and altitude, the country is divided into five standard physiographic regions, such as Terai, Siwaliks, Middle Mountains, High Mountains, and High Himalaya [35,36], which according to Duncan and Biggs [37] are further categorized into three broader zones, namely, Lowlands (Terai and Siwaliks), Mid-Mountains and Hills (Middle and High Mountains) and High Mountains (High Himalayas). Owing to such unique physiographical and topographical distribution, the country features a variety of climates that range from the tropical savannah over the southern plains to the polar frost in the northern mountains within a short horizontal distance of less than 200 km [38]. The population density is highest in the eastern lowlands region, followed by the regions of central lowlands, middle and eastern middle mountains, and western lowlands, respectively, while such density is lowest for the rest of Nepal.

There are four seasons in Nepal, namely, pre-monsoon (March–May), monsoon (June–September), post-monsoon (October–November) and winter (December–February). Pre-monsoon is characterized by hot, dry and westerly windy weather with mostly localized precipitation in a narrow band, whereas the monsoon is characterized by moist southeasterly monsoonal winds coming from the Bay of Bengal and occasionally from the Arabian Sea with widespread precipitation. Post-monsoon refers to a dry season with sunny days featuring a driest month, November. Winter is a cold season with precipitation mostly in the form of snow in high-altitude mountainous regions. Precipitation over Nepal is received by two major weather systems; the southwest monsoon greatly impacts the southeastern parts of the country during the monsoon season while the western disturbances predominantly affect the northwestern high mountainous parts during the winter season [39–43]. Similar to the monsoon season, precipitation during pre- and post-monsoon seasons is also generally higher towards the east [44]. In the Marsyangdi River basin (MRB) of Nepal, observed precipitation at the stations below 2000 m is mostly received in the form of rain while at the stations above this height, snowfall accounts for 17% ± 11% of the annual totals, where such a fraction rises with altitude [45].

Classifying the precipitation regimes of Nepal based on the shape and magnitude of monthly precipitation from 222 stations, Kansakar et al. [35] have illustrated that the precipitation patterns are mainly controlled by the orographic effect of the complex central Himalayan terrain and the east−west progression of the summer monsoon. Thus, owing to the intricate interaction amid the weather systems and their alteration by the extreme topographical variations (high mountains, valleys and river catchments), spatial distribution of precipitation in Nepal is highly heterogeneous (Figure 1a). For instance, the annual precipitation varies from less than 200 mm for the driest regions (Mustang, Manang, and Dolpa, located at the leeward-side north of the Annapurna) to above 5000 mm in and around the Lumle region. Two additional wetter regions with annual precipitation greater than 3500 mm are Num and Gumthang. On the other hand, regions of low precipitation typically also reside in the leeward-side of the Khumbu, Everest and other high mountainous regions [38,41,46]. Along the altitudinal extent of the central Himalayan region (~74°–88° E), the Tropical Rainfall Measuring

Mission (TRMM) precipitation dataset (1998–2005) indicates two parallel significant peak precipitation zones [47]; the first zone is at the mean elevation of ~0.95 km (mean relief of ~1.2 km) while the second one is at ~2.1 km (mean relief of ~2 km). Barros et al. [45] have suggested a weak altitudinal gradient of precipitation between 1000 and 4500 m altitude, whereas in deep river valleys with steep slopes, such a gradient of rainstorm is very strong. In general, they have found the maximum precipitation along the ridges and a strong east−west ridge-to-ridge precipitation gradient. Similar results were obtained from station-based observations in different regions of Nepal where precipitation peaks around 2500–3600 mm and decreases further with increase in altitude in high mountain regions [48–51].

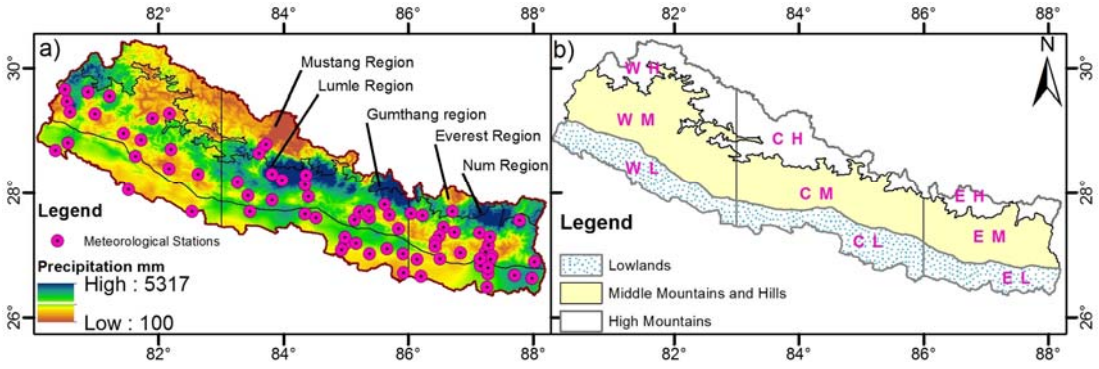

Figure 1. (**a**) Annual precipitation distribution (mm) over Nepal with precipitation pocket areas and dry areas delineated, and the meteorological stations used for the daily extreme analysis overlaid; (**b**) The three broader physiographic zones of Nepal and nine sub-regions (WL—Western Lowlands, WM—Western Middle Mountains and Hills, WH—Western High Mountains, CL—Central Lowlands, CM—Central Middle Mountains and Hills, CH—Central High Mountains, EL—Eastern Lowlands, EM—Eastern Middle Mountains and Hills, EH—Eastern High Mountains).

In addition to the horizontal and altitudinal precipitation gradients, a large seasonal precipitation gradient (~factor of 4) has also been observed over a short horizontal distance of ~10 km in MRB [52].

Precipitation does not feature long-term trends at seasonal and annual scales, except a localized trend in some parts of the Koshi River basin [44,53,54]. However, it features a significant relationship with the Southern Oscillation Index (SOI) [55]. Changes in the monsoonal precipitation regimes indicate the extension of the active monsoon duration mainly due to significantly delayed withdrawal, though the onset timing has been observed unchanged [56,57].

As the precipitation distribution is highly heterogeneous across the country, characterizing strong north−south and east−west gradients, the whole country is divided into nine sub-regions (Figure 1b) for regional field significance study. The latitudinal extent has been divided based on the demarcation of three broader physiographic regions, while for the longitudinal division, longitudes of 83° E and 86° E have been taken as the demarcation points (as used in [44]), yielding western, central and eastern regions, each containing three physio-geographic regions. For instance, the sub-regions within the western longitudinal belt are the western lowlands (WL), western middle mountains and hills (WM) and western high mountains (WH). The case for the central (CL, CM and CH) and eastern (EL, EM and EH) longitudinal belts is similar.

3. Data

We have obtained daily precipitation data from all available surface weather stations in Nepal that are being maintained by the Department of Hydrology and Meteorology (DHM), Nepal. These observations are consistent in terms of the measurement method as the obtained stations use the same type of US-standard 8-inch diameter manual precipitation gauges [58]. Though underestimated as in other types of gauges, these gauges can also measure snow water equivalent. For that, the snow deposited in the gauge is at first melted by pouring hot water and then measured as normal rainfall

measurement. In the DHM database, the longest precipitation record available since 1946 is from only three stations, although there are records from 23 stations since 1947, and from around 40 stations since 1950. Until 1956, the precipitation observations were available only from the stations located east of Kathmandu and particularly within the Koshi River basin. Afterwards, the number of precipitation stations considerably increased, reaching up to 100, 190, 240, 250, 370 and 410 by 1961, 1971, 1981, 1991, 2001 and 2010, respectively. However, all the available precipitation gauges do not feature regular data since the time of their inception [31]. For instance, among 450 stations that have been operational until recently, regular data of varying lengths from only around 400 stations either due to short-term discontinuity of the stations or their relocation are available (Figure 2). In order to ensure a balanced spatial distribution of stations across Nepal and employing the maximum common length of the high-quality continuous data available from the maximum number of stations, we have restricted the period of our daily extreme analysis to 1970–2012. Within such a period, the stations that feature data gaps for more than (1) a fortnight within a year; (2) four consecutive years or (3) for six years in total were excluded from the analysis.

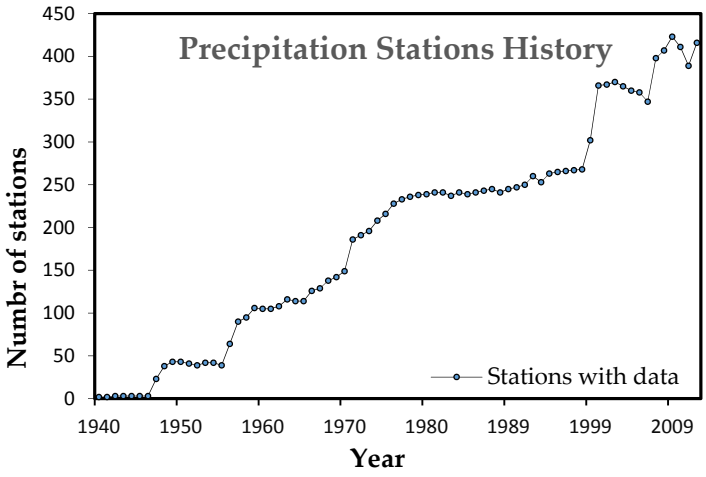

Figure 2. The number of precipitation gauges and their age in the Department of Hydrology and Meteorology (DHM) database.

The quality control of the data from the considered stations was performed using the RClimDex toolkit [59], which can identify potential outliers and negative precipitation values [4]. After the quality control, testing the homogeneity is the most important step [60] as it identifies the variations that occurred due to purely non-climatic factors, such as faults in the instruments or changes in the measurement method, aggregation method, station location, station exposure and observational practice [61]. The homogeneity test was performed for each station by monthly time series using the RHtest toolkit, which can statistically identify the multiple step changes by using a two-phase regression model with a linear trend of the entire time series [62]. Since the stations observe large Euclidean distances in complex mountainous terrains, we have performed a relative homogeneity test, without using a reference time series [63,64]. The inhomogeneity of a station has been decided based on the RHtest results, graphical examination and coincidence of known ENSO or localized precipitation events. The stations featuring any inhomogeneity were excluded from the analysis. Such strict station selection criteria have yielded the continuous, homogeneous, high-quality daily observations from only 76 stations for the 1970–2012 period. These 76 stations have been used for the computation of daily precipitation extremes (Figure 1a and Table 1) and seasonal precipitation total.

For sub-regions considered for field significance study, these stations ensure an adequate spatial distribution of stations at least across the middle mountain and lowland sub-regions. The number of stations that fall in each sub-region of WM, WL, CH, CM, CL, EM and EL are 14, 4, 3, 16, 11, 19 and 9, respectively. Since the stations within the western and central regions are relatively younger,

there are more stations within the eastern region that fulfill the selection criteria. As for high mountain sub-regions, long-term data was available only from CH, due to the low density of the high-altitude station network. Hence, we limit our sub-regional analysis to seven sub-regions only.

Table 1. List of meteorological stations.

Region	ID	Name	Lat (°)	Lon (°)	Height (m)
WL	106	Belauri santipur	28.683	80.35	159
	209	Dhangadhi (atariya)	28.8	80.55	187
	416	Nepalgunj Reg. off.	28.052	81.523	144
	510	Koilabas	27.7	82.533	320
WM	101	Kakerpakha	29.65	80.5	842
	103	Patan (west)	29.467	80.533	1266
	104	Dadeldhura	29.3	80.583	1848
	201	Pipalkot	29.617	80.867	1456
	202	Chainpur (west)	29.55	81.217	1304
	203	Silgadhi doti	29.267	80.983	1360
	206	Asara ghat	28.953	81.442	650
	303	Jumla	29.275	82.18	2366
	308	Nagma	29.2	81.9	1905
	402	Dailekh	28.85	81.717	1402
	404	Jajarkot	28.7	82.2	1231
	406	Surkhet	28.587	81.635	720
	504	Libang gaun	28.3	82.633	1270
	511	Salyan bazar	28.383	82.167	1457
CL	703	Butwal	27.694	83.466	205
	902	Rampur	27.654	84.351	169
	903	Jhawani	27.591	84.522	177
	907	Amlekhganj	27.281	84.992	310
	909	Simara airport	27.164	84.98	137
	910	Nijgadh	27.183	85.167	244
	911	Parwanipur	27.079	84.933	115
	912	Ramoli bairiya	27.017	85.383	152
	1109	Pattharkot (east)	27.1	85.66	162
	1110	Tulsi	27.013	85.921	251
	1111	Janakpur airport	26.711	85.924	78
CM	701	Ridi bazar	27.95	83.433	442
	722	Musikot	28.167	83.267	1280
	802	Khudi bazar	28.283	84.367	823
	804	Pokhara airport	28.2	83.979	827
	807	Kunchha	28.133	84.35	855
	808	Bandipur	27.942	84.406	995
	810	Chapkot	27.883	83.817	460
	814	Lumle	28.297	83.818	1740
	904	Chisapani gadhi	27.56	85.139	1729
	1008	Nawalpur	27.813	85.625	1457
	1015	Thankot	27.688	85.221	1457
	1022	Godavari	27.593	85.379	1527
	1023	Dolal ghat	27.639	85.705	659
	1029	Khumaltar	27.652	85.326	1334
	1030	Kathmanduairport	27.704	85.373	1337
	1115	Nepalthok	27.42	85.849	698
CH	601	Jomsom	28.78	83.72	2744
	604	Thakmarpha	28.739	83.681	2655
	607	Lete	28.633	83.609	2490

Table 1. *Cont.*

Region	ID	Name	Lat (°)	Lon (°)	Height (m)
	1112	Chisapani bazar	26.93	86.145	107
	1213	Udayapur gadhi	26.933	86.517	1175
	1216	Siraha	26.656	86.212	102
	1311	Dharan bazar	26.792	87.285	310
EL	1316	Chatara	26.82	87.159	105
	1319	Biratnagar airport	26.481	87.264	72
	1320	Tarahara	26.699	87.279	121
	1408	Damak	26.671	87.703	119
	1409	Anarmani birta	26.625	87.989	122
	1102	Charikot	27.667	86.05	1940
	1103	Jiri	27.633	86.233	2003
	1202	Chaurikhark	27.7	86.717	2619
	1203	Pakarnas	27.443	86.569	1944
	1204	Aisealukhark	27.36	86.749	2063
	1206	Okhaldhunga	27.308	86.504	1731
	1207	Mane bhanjyang	27.215	86.444	1528
	1210	Kurule ghat	27.136	86.43	341
	1211	Khotang bazar	27.029	86.843	1305
EM	1303	Chainpur (east)	27.292	87.317	1262
	1305	Leguwa ghat	27.154	87.289	444
	1306	Munga	27.05	87.244	1457
	1307	Dhankuta	26.983	87.346	1192
	1308	Mul ghat	26.932	87.32	286
	1309	Tribeni	26.914	87.16	146
	1322	Machuwaghat	26.938	87.155	168
	1325	Dingla	27.353	87.146	1169
	1403	Lungthung	27.55	87.783	1780
	1410	Himali gaun	26.887	88.027	1654

Note: WL (western lowlands), WM (western middle mountains and hills), WH (western high mountains), CL (central lowlands), CM (central middle mountains and hills), CH (central high mountains, EL (eastern lowlands), EM (eastern middle mountains and hills) and EH (eastern high mountains)).

In addition to a daily extreme precipitation trend analysis, we present spatial variability maps of mean seasonal and of physically relevant daily precipitation extreme indices from the maximum number of stations that have the data for at least 20 years in the recent normal period (1981–2010) but two stations from high altitude (>3500 m) with only five years of data are also included to represent the high-altitude spatial pattern. Since these indices do not require the high-quality data, around 210 precipitation stations were considered for this analysis.

4. Methodology

4.1. Precipitation Indices

We have considered the extreme precipitation indices that are developed and recommended by the Expert Team on Climate Change Detection, Monitoring and Indices (ETCCDMI), jointly established by the World Meteorological Organization (WMO) Commission for Climatology and the Research Programme on Climate Variability and Predictability (CLIVAR) (Table 2). Based on the calculation method, these indices fall into four groups [65,66], namely, absolute indices, threshold indices, duration indices and percentile-based threshold indices.

Table 2. The description of ETCCDMI (Expert Team on Climate Change Detection, Monitoring and Indices).

Category	ID	Name of Index	Definition	Unit
HIP	R95	Very wet days	Annual total precipitation of days in >95th percentile	mm
HIP	RX1day	Max 1-day precipitation amount	Annual maximum 1-day precipitation	mm
HIP	RX5day	Max 5-day precipitation amount	Annual maximum consecutive 5-day precipitation	mm
HIP	R99	Extremely wet days	Annual total precipitation of days in >99th percentile	mm
FP	R10	Number of heavy precipitation days	Annual count of days when precipitation is ≥10 mm	Days
FP	R20	Number of very heavy precipitation days	Annual count of days when precipitation is ≥20 mm	Days
DWS	CDD	Consecutive dry days	Maximum number of consecutive dry days (precipitation <1 mm)	Days
DWS	CWD	Consecutive wet days	Maximum number of consecutive wet days (precipitation ≥1 mm)	Days
EX	WD	Annual wet/rainy days	Annual count of days when precipitation is ≥1 mm	Days
EX	PRCPTOT	Annual total wet-day precipitation	Annual total from days ≥1 mm precipitation	mm
EX	SDII	Simple daily intensity index	Ratio of annual total to WD in a year	mm/day

Note: HIP: High-intensity-related precipitation extreme, FP: Frequency-related precipitation extreme, DWS: Dry and wet spell or duration, EX: Extra.

The absolute indices include the annual maximum of 1-day and 5-day precipitation referred to as RX1day and RX5day, respectively. Threshold indices comprise of numbers of (1) heavy precipitation days (R10) and (2) very heavy precipitation days (R20). R10 (R20) denotes the counts of days in a year when precipitation was ≥10 mm (≥20 mm). The duration indices encompass the consecutive wet and dry days (CWD and CDD), which describe the maximum lengths of consecutive wet and dry days, respectively. Unlike the absolute threshold-based indices, percentile-based indices better represent the spatial aspects of precipitation extremes, accounting for spatial heterogeneity of precipitation. However, different researchers have used different percentiles as thresholds for defining such extremes. For example, Krishnamurthy et al. [18] and Bookhagen [67] have used the 90th percentile, Duncan et al. [29] and Casanueva et al. [68] have used the 95th percentile and Alexander et al. [4], Klein Tank et al. [5], Donat et al. [14], and Sheikh et al. [11] have used the 95th and 99th percentiles. Here, the percentile-based threshold indices include two; the yearly total precipitation from very wet days (R95) and extremely wet days (R99) observing above than 95th and 99th precipitation percentiles, respectively. Since R95 and R99 indices are based on the long-term percentile thresholds, they may differ from station to station but not on an inter-annual scale. Three additional indices that do not fall in any of the above categories are the annual wet days (WD) described as the annual count of days when precipitation was ≥1 mm, annual total precipitation from WD (PRCPTOT) and the simple daily intensity index (SDII) defined as the ratio of PRCPTOT to WD within a year. These indices were computed using the RClimDex toolkit [59] while the regionalization of the physically relevant indices has been performed using Global Kriging interpolation (See [38] for details).

The considered extreme precipitation indices are mainly the indicators of floods and droughts or indirect indicators which in combination with the main indicators provide valuable information. For instance, R95, R99, RX1day and RX5day indices characterize the magnitude of very intense precipitation events that trigger flash floods and landslides. R10 and R20 assess the frequency of heavy and very heavy precipitation events. On the other hand, CDD and CWD indirectly provide the indication of droughts, which is quite important for the agricultural activities [68]. The SDII, PRCPTOT and WD indirectly provide useful information when combined with other extreme indices. Therefore, we have presented and discussed the results in four broad categories, namely, high-intensity-related precipitation extreme (HIP) indices which consist of absolute and percentile-based threshold indices, frequency-related precipitation extremes or threshold-based (FP) indices, dry and wet spell or duration (DWS) indices and extra indices (EX) (Table 2).

In addition to the computation of extreme precipitation indices, the temporal changes in these indices and seasonal total precipitation have also been assessed. For this, trends in the considered indices (except R99) were analyzed using the Mann−Kendall (MK) trend test [33,34] while the magnitude of trend was estimated using the Theil−Sen's (TS) slope method [69,70]. Trend assessment for R99 was possible, but no trends were found for more than half of the stations due to large inter-annual variability that resulted in zero values for more than half of the R99 time series. They were therefore, excluded from the analysis.

4.2. Trend Analysis

4.2.1. Mann−Kendall Trend

The MK trend test [33,34] has been widely used to assess the significance of a trend in the time series as the test does not require normally distributed data sets [71,72] and can cope with missing data records and extremes.

4.2.2. Theil−Sen's Slope

If a linear trend is present in a time series, the true slope of the existing trend can be computed using the non-parametric TS approach. This test is widely used and robust as it is less sensitive to outliers and missing values in data [69,70].

4.2.3. Trend-Free Pre-Whitening

The MK test is based on the assumption that the time series is serially independent. However, often the hydro-meteorological time series contain a serial correlation [73–75], affecting the MK test results. For instance, existence of a positive (negative) serial correlation in a time series overestimates (underestimates) the significance of the MK test (e.g., [74,76]). To limit such effect of serial correlation on the MK test results, several pre-whitening (PW) procedures have been proposed [71,75–77] including trend-free pre-whitening (TFPW). TFPW more effectively reduces the effect of a serial correlation present within the hydro-meteorological time series on the MK test results [78–80]. Here, we have used TFPW as proposed by Yue et al. [74].

In TFPW, the initial step is to estimate the true slope of a trend using Sen's slope method, unitize the time series by dividing each sample with the sample mean and de-trend the time series. The lag-1 auto-correlation is then estimated and removed if existing and the time series is subsequently blended back to the pre-identified trend component. Finally, the MK test is applied to pre-whitened time series (see [74,75] for further information).

4.2.4. Field Significance

A certain region can feature a number of stations with positive or negative trends. Thus, the field significance test is used to identify regions with trends of a consistent sign, independent of statistical significance of the individual station trends [81,82].

Various methods are available for assessing the field significance of local trends [71,73,74,83–86]. We have adopted the method of Yue et al. [74] to assess the field significance in the seven sub-regions (Figure 1b) with sufficient data. In this method, the original station network has been resampled 1000 times with the bootstrapping approach [87], distorting (preserving) the auto-(cross-)correlation to avoid its influence on the field significance analysis. The MK test is then applied to synthetic time series of each site. At the given significance level, the numbers of sites with significant upward trends and downward trends, respectively, have been counted using Equation (1) for each resampled network.

$$C_f = \sum_{i=1}^{n} C_i \quad (1)$$

where, n, indicates the number of stations within a region of analysis and C_i refers to a count of statistically significant trends (at 0.1 level) at the station, i. This procedure has been repeated 1000 times for each resampled network. Ranking the corresponding 1000 values of counts of significant positive (negative) trends in an ascending order using the Weibull [88] plotting position formula yields the empirical cumulative distributions, C_f, as:

$$P\left(C_f \leq C'^{r}_{f}\right) = r/(N+1) \tag{2}$$

where, $_r$, is the rank of C and N is the number of resampled networks. The probability of a number of significant positive (negative) trends in the original network has been estimated by comparing with Cf of significant positive (negative) trends obtained from the resampled networks (Equation (3)).

$$P_{\text{obs}} = P\left(C_{f,\,\text{obs}} \leq C'^{r}{}_{f}\right) \text{ where } P_f = \begin{cases} P_{obs}, & \text{for } P_{obs} \leq 0.5 \\ 1 - P_{obs}, & P_{obs} > 0.5 \end{cases} \tag{3}$$

At the significance level of 0.1, if $P_f \leq 0.1$, then the trend over a region was considered significant. A similar approach has been employed by Petrow and Merz [89] for assessing the field significance of flood time series in Germany and by Hasson et al. [63] for hydro-meteorological time series in the Hindukush-Karakoram-Himalayan region of the upper Indus basin.

5. Results and Discussion

5.1. Spatial Distribution of Mean Seasonal and Daily Precipitation Indices

In addition to the seasonal mean precipitation distribution, spatial patterns of mainly the high-intensity- and frequency-related extremes (R95/R99 percentile precipitation, RX1day and WD, R10, R20, respectively), which are relevant for water resources, as well as flood and agriculture management, are computed from 210 stations over the period of 1981–2010 (Figures 3 and 4).

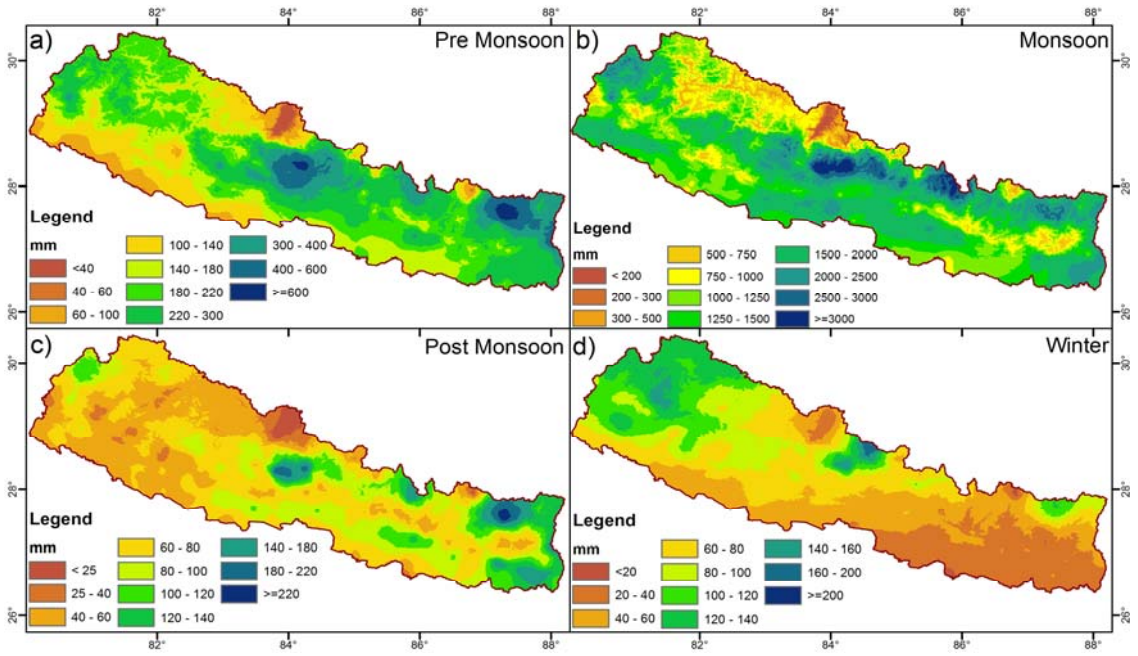

Figure 3. Spatial distribution of mean seasonal precipitation (mm) for (**a**) Pre monsoon; (**b**) Monsoon; (**c**) Post monsoon; and (**d**) winter season over the period of 1981–2010. Note: Legend scale of all four seasonal maps are different.

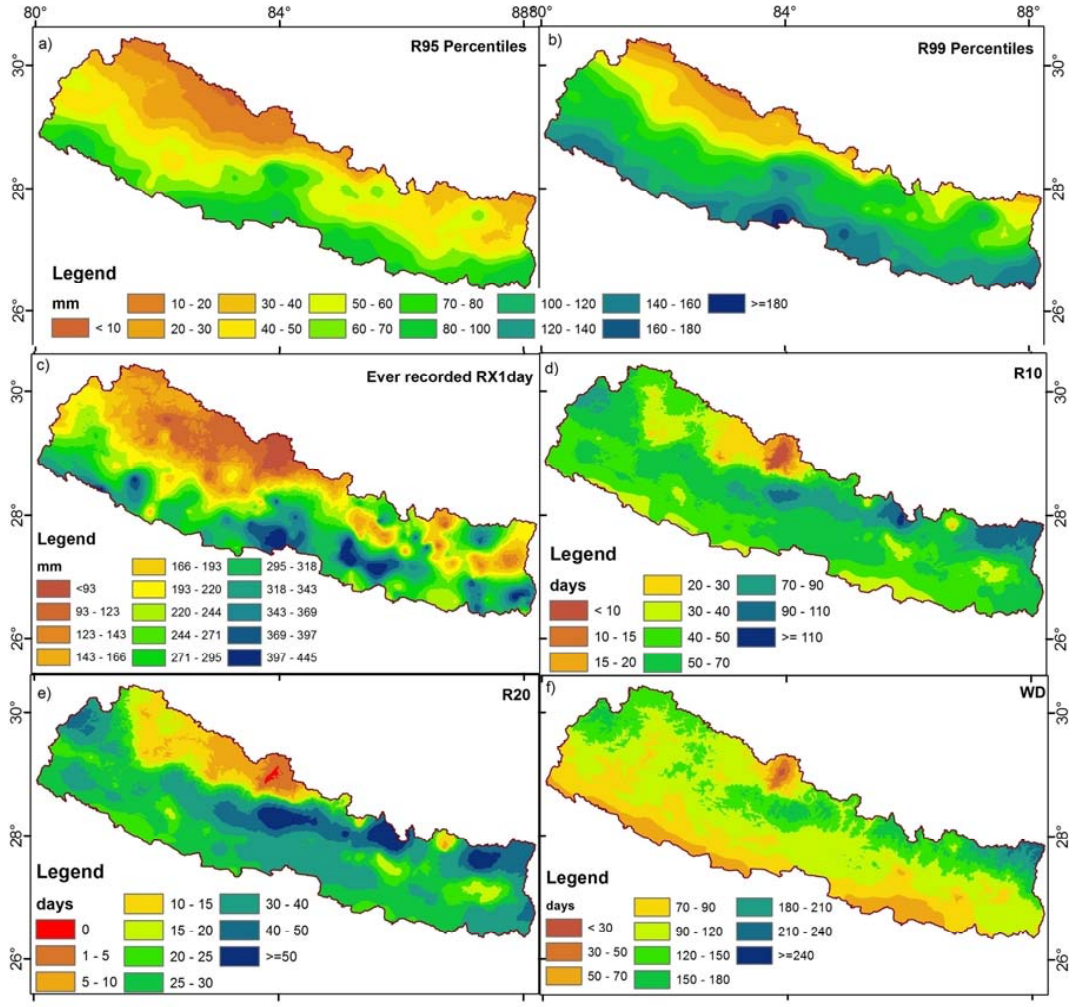

Figure 4. Spatial distribution of (**a**) 95th percentile; (**b**) 99th percentile mean values of daily precipitation; (**c**) ever-recorded one-day extreme precipitation; (**d**) mean annual number of days with precipitation ≥10 mm; (**e**) mean annual number of days with precipitation ≥20 mm (**f**) mean annual number of days with precipitation ≥1 mm (wet/rainy days) over the period of 1981–2010. Note: Legend scales are different.

The monsoonal precipitation dominates annual precipitation with contribution of around 80% of the annual precipitation, whereas precipitation during winter, pre- and post-monsoon seasons contribute only 3.5%, 12.5% and 4.0%, respectively [90]. Therefore, monsoonal precipitation distribution (Figure 3b) is similar to the annual precipitation distribution (Figure 1a and [38]), indicating three high-precipitation pocket areas around Lumle, Gumthang and Num that receive more than 3000 mm of monsoonal precipitation. On the other hand, dry leeward regions are in Mustang, Manang and Dolpa, featuring the lowest precipitation amounts of less than 150 mm. These findings are consistent with Böhner et al. [42], who reported that the regions north of high mountains are drier (<500 mm) in general and, depending on the alignment of surrounding mountain ranges, river valleys and the valleys lying in middle mountains and hills are also relatively drier (500–1000 mm) than surrounding mountain slopes and ridges. Such a pattern is more pronounced in the lower reaches of the river valleys, which lie between the southern frontal mountains and northern elevated mountain range. Such comparatively dry valleys are distinct in the surroundings of Tamor at Mulghat, Arun at Leguwaghat, DudhKoshi at Kuruleghat, Tamakoshi at Manthali, Sunkoshi at Nepalthok, Pachuwarght and Dolalghat, Bheri at Rakam and Dunai, Karnali at many upper river valleys (Jumla, Thirpu, Nagma, Gamshreenagar, etc.), Seti at Dipayal, Mahakali at Binayak and all other river valleys that lie north

of tall mountain ranges (Figure 3b). On the other hand, as demonstrated earlier based on satellite data [47], precipitation is high (1500–2500 mm) on the windward side of both mountain ranges that lie north and south of such river valleys, creating double-peaked rainfall bands from south to north. In contrast to the river valleys lying within the northern elevated mountain range and southern frontal mountains, the majority of river valleys in Pokhara (near Lumle) and the surrounding region receive abundant (>1250 mm) monsoonal precipitation.

The precipitation in pre-monsoon, monsoon and post-monsoon seasons, more or less, follows the same spatial pattern in terms of representing three-peak precipitation pocket areas, as well as an east to west gradient. Pre-monsoon precipitation, mostly associated with thunderstorms, is very low in CH and the western half of the lowlands. There is a variation from less than 100 mm in WL, CH and in some areas on the leeward side of high mountains in the eastern region, to more than 700 mm in precipitation pocket areas and eastern mountains. Post-monsoon is the transition season between monsoon and winter. Therefore, following the retreat of monsoon from west to east, the western half of the country remains very dry, receiving below 40 mm of precipitation, whereas it is more than 200 mm in the eastern mountainous region. In contrast to other seasons, winter precipitation is higher over WM (>200 mm) and in a few isolated wet pockets in the central and eastern high mountainous regions. Winter precipitation is lowest over eastern lowlands (<20 mm) and feature a clear west to east as well as north to south gradient (Figure 3d). Our seasonal spatial maps are broadly similar to the previous studies for all of Nepal [29,44,90]; however, the inclusion of a large number of stations with the improved spatial interpolation technique has resulted in a much finer and realistic representation.

Contrary to the distribution of annual precipitation (Figure 1a), suggesting three rainfall pockets in Nepal, high values of extreme percentile thresholds are found in the lowlands (Terai and Siwalik), while low values are found in the highland regions (Figure 4a,b). For instance, annual mean of R99 percentile threshold in the lowlands is around 150 mm, whereas it is only about 30 mm in the highlands. Interestingly, the spatial pattern of R99 is quite similar to R95, and to some extent, to ever-recorded RX1day (Figure 4c). The high values of extreme thresholds in lowlands are associated with fewer heavy rainfall events (Figure 4a,b), while their relatively lower values observed in the middle mountains—despite the high annual precipitation (Figure 1a)—are due to weak but persistent rainfall [45,91]. The ever-recorded one-day maximum precipitation (RX1day) is found lowest in the central highlands followed by western highlands, whereas it is highest in the central lowlands followed by eastern and western lowlands. These spatial patterns are broadly similar to RX1day mapping using ground observation [92,93] and 90th percentile threshold mapping using TRMM data set [67]. The overall high values of R95, R99 and RX1day over lowlands suggest that these regions are more prone to soil erosion, landslides, flash flooding and subsequent inundations.

Unlike R95, R99 percentiles, and ever-recorded RX1day, spatial patterns of WD, R10 and R20 are largely similar to the annual distribution of precipitation. WD is lowest (below 40 days) in the very dry region of Mustang while it is highest (above 180 days) in EH followed by CM, WH and WM regions (Figure 4f). On average, WD is around 100 days over the lowlands and around 140 days over high and middle mountains. Similar to WD, R10 is lowest over Mustang, featuring only less than 11 days whereas R10 is above 110 days for the EH region (Figure 4d). On average, R10 is around 70 days over most of Nepal. R20 is almost zero over the dry Mustang region and at the minimum over WH and CH as these regions rarely experience very heavy precipitation events. However, over EH and CM regions and particularly over the high precipitation pockets, R20 is more than 50 days (Figure 4e). On average, R20 is around 40 days across the whole country. Interestingly, from Figure 4, it can be clearly noted that the frequency-related extreme indices of WD, R10 and R20 feature quite an opposite north−south gradient compared to high-intensity-related extreme indices of R95/R99 percentile precipitation and ever-recorded RX1day, with few sporadic exceptions.

The large spatial heterogeneity of mean precipitation across the country in different seasons indicates the requirement of localized information for water resources management and planning. Terai, Siwalik and river valleys, for example, are more prone to flood disaster, while mountains and

hills face a higher landslide risk. The R95 and R99 thresholds computed here can also be directly utilizable for fixing the thresholds for flood warnings in different regions of Nepal.

5.2. Trend Analysis

In addition to the spatial distribution of mean precipitation and extreme indices, their time evolutions have been analyzed in order to see how these indices are changing over time. For this, trend slopes from the individual stations, their field significance for the seven geophysical sub-regions of Nepal along with the summary of these trend features are shown in Figures 5–9. The stationwise trends and percentages of the negative/positive trends along with their significance are also additionally included in Supplementary Materials Table S1.

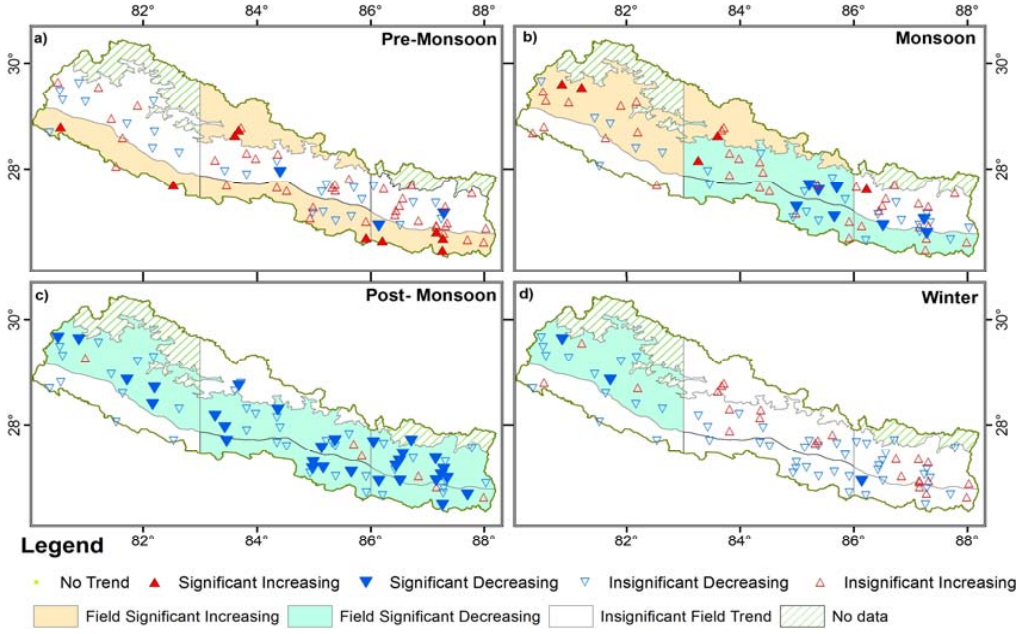

Figure 5. Stationwise and field significant trends of seasonal precipitation total for (**a**) Pre monsoon; (**b**) Monsoon; (**c**) Post monsoon; and (**d**) Winter season (significance at 0.1).

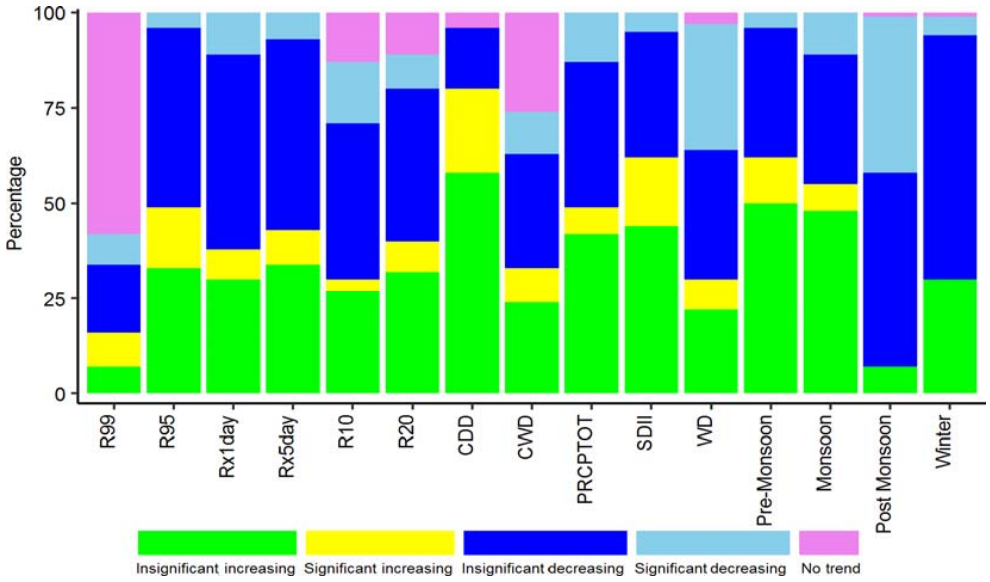

Figure 6. Percentage (from total stations) of stations with different trend features in Nepal.

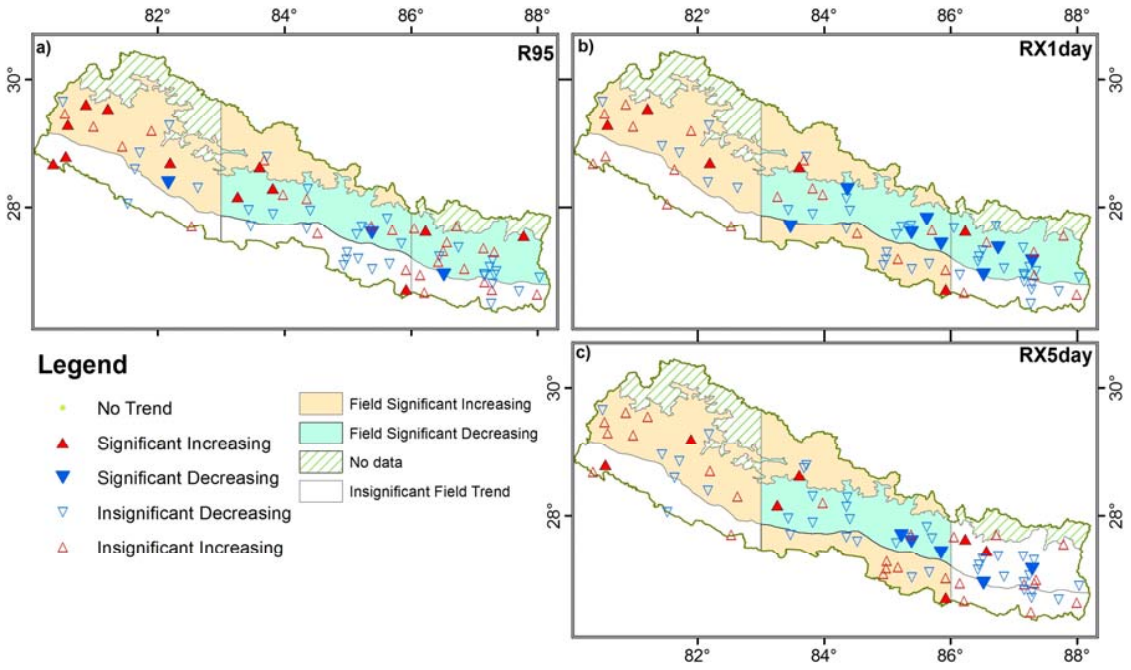

Figure 7. Stationwise and field significant trends for (**a**) R95; (**b**) RX1day; and (**c**) RX5day extreme precipitation indices (significance at 0.1).

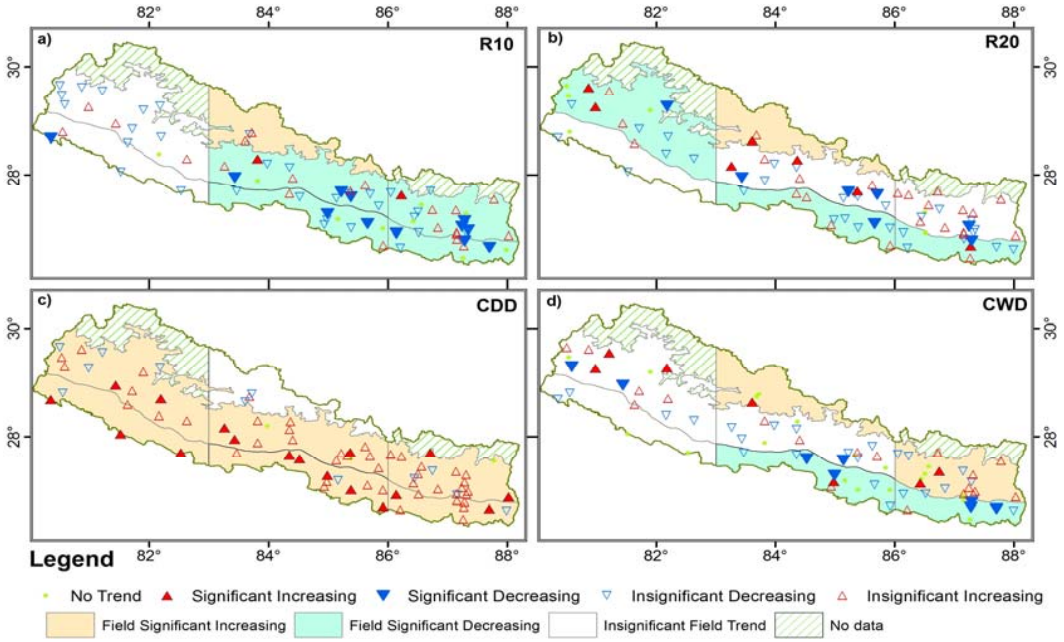

Figure 8. Stationwise and field significant trends for (**a**) R10; (**b**) R20; (**c**) CDD; and (**d**) CWD indices (significance at 0.1).

5.2.1. Seasonal Precipitation

All stations show a mixed pattern of increasing and decreasing trends for the pre-monsoon precipitation across Nepal (Figure 5a). However, around 62% of the total stations feature a rising trend, where such a trend is significant only at around 12%. Most of these stations are mainly concentrated within EL, CL, WL and CH regions. Only 4% of the total stations suggest a significant decreasing trend in pre-monsoon precipitation (Figure 6). The results of field significance analysis are also

congruent with the stationwise trends, indicating a significant rise in pre-monsoon precipitation over WL, CL, EL and CH. These findings are mostly consistent with Duncan et al. [29] who have shown a countrywide precipitation rise. For the field insignificant middle mountain regions, differences with Duncan et al. [29] may arise due to employing distinct observational datasets and methodology. Since pre-monsoon precipitation is mostly accompanied with thunderstorms as evident heavily over EL [94], rise in the pre-monsoon precipitation over lowlands and CH regions will increase the extremely intense thunderstorms. Further, an increase in the pre-monsoon precipitation indicates changes in the seasonality of the precipitation regime over such regions [95,96].

The monsoon precipitation features a mixture of drying and wetting trends (Figure 5b). About one-fifth of the total stations exhibit significant trends with around 11% negative and 7% positive trends (Figure 6). The significant negative trends are concentrated in the central and eastern parts while significant positive trends are found in WM and CH regions. Field significance analysis more clearly suggests the rising and falling trends of monsoonal precipitation over the designated regions. For instance, increase in monsoonal precipitation is significant over the WM and CH regions whereas decrease is significant over CM, CL and EL regions, largely consistent with the signals observed at the local stations. Since the monsoonal precipitation is very important for summer crops (paddy, maize and millet), which constitute around 80% of the total national cereal production in Nepal [56], decreasing monsoonal precipitation may significantly affect the yield of cereal crops, as a significant decrease in the yield of rice has already been reported for the years of below-normal monsoonal precipitation [97].

Interestingly, most of the stations (92%) show a decrease in the post-monsoon precipitation, where such a signal is statistically significant at 41% of the total number of station. Decreasing post-monsoon precipitation is further suggested by the field significant decrease in all regions except for WL and CH (Figure 5c). This is in agreement with the findings of Khatiwada et al. [98], who have also indicated a decreasing post-monsoon precipitation over the Karnali basin in western Nepal for the 1981–2012 period. Over the same period, a significant decrease in precipitation during the post-monsoon dry months of November and winter season month December was also noticed in the Gandaki river basin of Nepal [57,99]. The observed decreasing post-monsoon precipitation may adversely affect the production of paddy crop, as it enters into sensitive stage of spikelet formation, fruiting and ripening, requiring more water during the post monsoon season [100].

Similar to post-monsoon precipitation, most of the stations feature a negative trend (68%) for winter precipitation over Nepal. However, such a negative trend is statistically significant at only 4% of the total stations, mainly lying within the WM region. Field significance analysis also suggests a significant decreasing trend for the winter precipitation over WM (Figure 5d). Khatiwada et al. [98] have also reported a decreasing winter precipitation over the Karnali basin in western Nepal for the 1981–2012 period. Based on GPCP and satellite-based datasets, Wang et al. [101] have likewise identified declining winter precipitation over the western region of Nepal in recent decades. Consistently, weakening influence of the western disturbances over the central Himalayas has also been found [102], and in line with this, decreasing winter precipitation has been reported in the adjoining western Himalayan region in India [103]. Further, Wang et al. [101] have attributed this decline to three main factors: (1) decadal trend towards negative phase of arctic oscillation in recent decades that has created a local mass flux circulation with descending branch over western Nepal; (2) the Indian ocean warming, and; (3) the anthropogenic aerosol loading. It is pertinent to mention that the winter precipitation, though low in volume, plays an important role in meeting the water demand of the winter crops and in feeding the rivers through accumulating their headwaters with snow that melts during the dry pre-monsoon season [42]. Particularly for the western hills and mountainous regions where food production is largely dependent upon rain-fed agriculture, decreasing winter precipitation may affect the winter crop production [101] of wheat, barley and potatoes, a major crop of the hills and mountains. Moreover, the decreasing winter precipitation in the region, where winter precipitation is substantially higher than in other regions, could also lead to a reduction in pre-monsoon season river flows, which are largely dependent on the snow and glacier melt during the dry season.

5.2.2. High-Intensity-Related Precipitation Extremes

The stationwise trends of R95 (total annual precipitation from the days of a year featuring >95 percentile precipitation) and RX1day and RX5day (annual maximum 1-day and 5-day precipitation) indices, along with their field significance, are shown in Figure 7.

The analysis reveals a mixture of equally increasing and decreasing trends in R95 across Nepal with only one-fifth of the total stations featuring significant trends. For instance, around 16% of the total stations show a significant positive trend in R95 while only 4% show its significant negative trend (Figure 6). The stations featuring a statistically significant rise in R95 are mainly concentrated within the western part of the country. Rising trends in R95 at local stations are found field significant over the WM and CH regions, while falling trends in R95 are field significant over the CM and EM regions.

For RX1day indices, about 60% of the analyzed stations feature falling trends and around one-tenth of the total stations show such a falling trend as significant. A large number of stations showing falling RX1day are located in CM and EM regions. In contrast, stations in the western region (WL and WM) have a higher number of increasing trends for RX1day. Similar to RX1day, a higher number of negative trends in RX5day is observed within CM and EM regions, while more positive trends are found in the western regions (WL and WM). Field significance results are largely in agreement with the stationwise trends. Positive trends in RX1day and RX5day are field significant over the WM, CL and CH regions, while negative trends are field significant over the CM region and RX1day decrease is additionally field significant over the EM region. Such a pattern of change in RX1day is consistent with the previous studies [32,104] that also report a decreasing trend of RX1day from most of the stations, where such a trend is particularly significant above 100 m (asl) within the Koshi River basin—a basin spanning mainly over the eastern and partially over the central region of our study area.

In summary, all three indices of R95, RX1day and RX5day feature a field significant rising trend over the WM and CH regions, whereas over the CL region, only the latter two are field significant. Decreasing trends in R95, RX1day and RX5day are found field significant over the CM region, while the former two are additionally field significant over the EM region. Coherence amid field significance rising trends of all three intensity-related extreme precipitation indices together with the dominance of stationwise significant rising trends over WM and CH regions indicate that precipitation extremes might be more intense in the near future.

On the other hand, decreasing field significant trends of all three indices over the CM region and of two indices, R95 and RX1dy, over the EM region indicate to some extent the weakening of intense precipitation extremes over such regions.

Since our analysis period is only until 2012, occurrence of extreme events during 14–17 June 2013 in Uttarkhanda, India and the bordering areas of western Nepal, and the 14–16 August 2014 event in western Nepal indicates the continuation of this pattern in the western region of Nepal. Further, Cho et al. [105] attributed the increase in extreme precipitation events like that of Uttarkhanda and the bordering region of western Nepal in recent decades to an amplification of an upper tropospheric mid-latitude shortwave trough pattern in the northern region of South Asia due to the increase in greenhouse gases and aerosols. In general, this kind of amplification in association with west–northwestward migration of monsoon low creates the highly favorable environment for vigorous interaction of tropical (monsoon) and extra-tropical (mid-latitude) circulation resulting in extreme precipitation events in the western Himalayan region [106]. Thus, the western mountainous region of Nepal lying at a higher latitude and being an adjacent region of western Himalayas could have greater influence of such mid-latitude wave train pattern, whereas opposite or no influence of that pattern can occur towards eastern region. However, the shortwave train pattern was analyzed only for June and no conclusions could be made for whole monsoon season during which extreme precipitation events occur.

In addition, physical mechanism responsible for enhancement of monsoon precipitation and extremes towards the central and eastern region of foothills of Himalayan region are normally associated with break/active monsoon condition in mainland India/Himalayan foothills (north ward

migration of monsoon trough towards foothills of Himalaya from its normal position) during which interaction of southward migration of extratropical westerly troughs (dry air subsidence in Indian subcontinent at mid-to-upper troposphere) and weak monsoon circulation takes place [107]. The detail analysis of changing pattern of break monsoon situation and other physical mechanism responsible for changing extreme precipitation pattern over the whole monsoon season for Nepal is still lacking and it could be far from simple as the complex interaction of global, synoptic scale weather systems and topography takes place in the monsoon dominated region producing localized extreme precipitation.

The increasing intense precipitation over western mountainous region indicates higher risks of soil erosion and landslides in the fragile mountainous regions which are extremely vulnerable to these disasters due to manmade activities—deforestation for settlement, road network and agricultural activities—or natural causes like earthquakes. Lacking adaptive capacities of the remote mountains and hills further aggravate the situation. Additionally, increasing intense precipitation events in these regions consequently increases the risk of floods and inundation in densely populated river valleys and southern lowlands, destroying life and property, and causing damages to the agricultural land thereby impacting the socioeconomic development.

Nevertheless, absence of increasing trend of extreme intense precipitation in the central region where land is highly ruptured with recent earthquake still requires suitable adaptive measures to reduce the risk of landslides in the regions, as continuous but low intensity and even normal extreme threshold precipitation values of rainfall can easily trigger such disasters in the region.

5.2.3. Frequency-Related Precipitation Extremes

Since days with 10 mm and 20 mm precipitation events are quite common during the monsoon season over many parts of Nepal (Figure 4d,e), these events which are typically defined as heavy and very heavy precipitation in fact represent only moderate precipitation events over large areas of Nepal. Our results show a mixed pattern of stationwise increasing and decreasing trends for R10 (annual number of days with $\geq$10 m) across Nepal. However, around 57% of the total stations show a negative trend, which is significant at around 16% of the stations mostly concentrated in the central and eastern regions (Figure 6). Field significance test results also suggest the same, exhibiting significant negative trends for the CM, EM, CL and EL regions (Figure 8a). The pattern of change in R20 (annual counts of days when Precipitation is $\geq$20 mm) likewise indicates a mixed response with approximately equal numbers of rising and falling trends (Figure 8b). However, R20 is significantly decreasing for the regions of CL, EL and WM and significantly increasing for the region of CH. Further, coherent decrease in R10 and R20 over CL and EL clearly suggests a decrease in the number of moderate precipitation events over the respective regions.

5.2.4. Dry and Wet Spells

The analysis of CDD (consecutive dry days) indices suggests a widespread increase in the dry period over the whole country (Figure 8c). Around 80% of the analyzed stations exhibit an increase in CDD over the period of 1970–2012, though this trend is significant only at 22% of the total (Figure 6). In line with the stationwise trends, field significance trends are also statistically significant for all the sub-regions, except for CH. This finding is consistent with previous studies of Shrestha et al. [32] and Sigdel and Ma [104] over Koshi basin of Nepal. A similar increase in CDD has also been reported for the Songhu River basin in China [108] and across Bangladesh [109], as CDD is mostly related to the large-scale weather systems rather than localized systems [68].

The CWD (consecutive wet days) also reveals a mixed pattern (Figure 8d). However, the field significance analysis suggests a significant decreasing trend for CL and EL regions but a significant increasing trend for EM and CH regions. The CWD changes are mainly observed during the monsoon season; hence, such changes do not necessarily corresponds to changes in CDD, which are observed mostly in the dry seasons.

It is worth mentioning that duration and occurrence-related indices of CDD and CWD can only indirectly characterize the drought, which is a complex phenomenon and depends upon many other factors besides precipitation. Nevertheless, increasing CDD observed over the study area is consistent with the most widespread and worst drought observed in recent decades across the country [99,101,110,111]. Rise in CDD clearly indicates the prolongation of the dry period across the country, implying certain changes in the seasonality of prevailing precipitation regimes [95,96]. Further, this increase in the dry period can negatively impact crop yield and hydropower generation and can, moreover, elevate respiratory-related health problems in Nepal by increasing the concentration of particulate matter in the air. Since the frequency and scale of the forest fires in Nepal and other regions are also strongly related to the length of dry spells [112], the rise in CDD will aggravate such events, endangering wildlife and causing huge socioeconomic losses.

5.2.5. Extra Indices (PRCPTOT, SDII and WD)

One-fifth of the total number of stations exhibit significant trend changes in PRCPTOT. Around 13% of stations suggest a significant falling trend while 7% of stations suggest a significant increasing trend (Figure 6). The majority of statistically significant negative trends are concentrated in the central and eastern parts while higher numbers of significant positive trends are observed in the western parts of the country (Figure 9a). Interestingly, the stations above 29° N reveal an increasing trend while those below this latitude features a decreasing trend. The field significance test also indicates a significant decrease in PRCPTOT over CM, CL, EM and EL regions and a significant increase over WM and CH regions. The increasing trend in WM is consistent with Baidya et al.'s [28] findings for the western region. The spatial pattern of trend changes in PRCPTOT is quite similar to that of the monsoonal precipitation as it dominates (about 80% of) the total annual precipitation in Nepal. Decreasing PRCPTOT over the eastern region that covers most of the Koshi River basin within Nepal is consistent with the reports of significant precipitation decrease over the Koshi River basin during the 1994–2013 period [50] and over the middle mountains and hills during the 1975–2010 period [32]. Based on the coarse resolution Global Precipitation Climatology Project (GPCP) dataset, Yao et al. [113] have also provided evidence of decreasing precipitation over all the Himalayas and an increase in the eastern Pamir regions during 1979–2010.

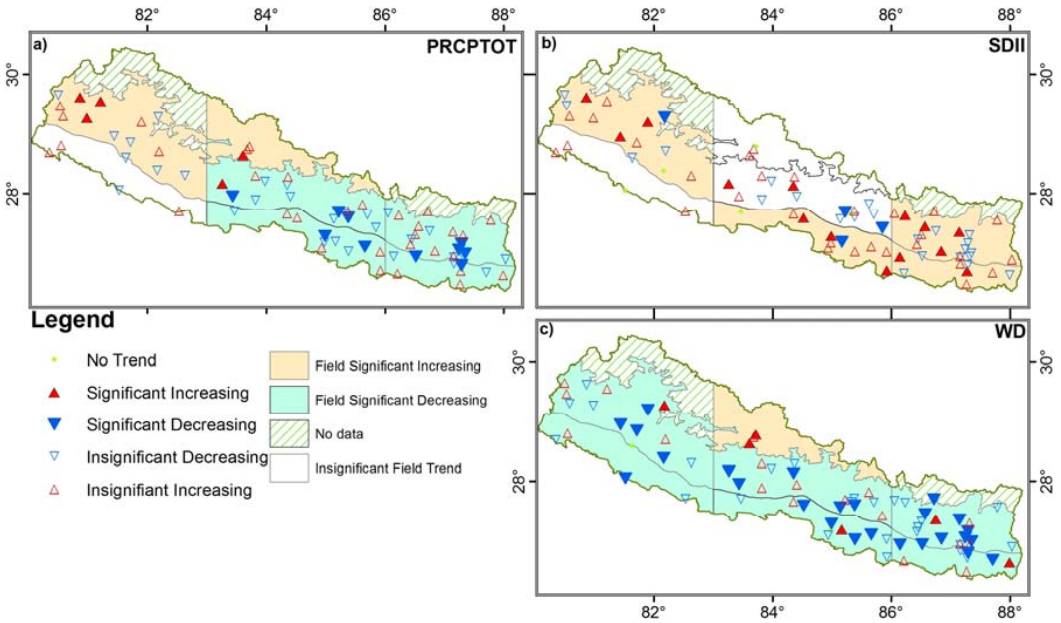

Figure 9. Stationwise and field significant trends for (**a**) PRCPTOT; (**b**) SDII; and (**c**) WD indices (significance at 0.1).

Notably, WD (wet days/rainy days) is decreasing (at 67% of the stations) across most of Nepal with a statistically significant decreasing pattern at one-third of the stations. Additionally, the individual stations' trends are also consistent with the field significant trends for all sub-regions, except for CH (Figure 9c). These findings are further consistent with the regional pattern of decreasing number of wet days over the whole of Southeast Asia [114].

The simple daily intensity index (SDII), defined as the ratio of PRCPTOT to WD, exhibits a positive trend (60% of the stations) across Nepal with statistically significant increasing trends at 14 stations (18%) and significant decreasing trends at four stations. Unlike significant decreasing trends in PRCPTOT over EM, EL and CL regions, in accord with Shrestha et al. [32], SDII features a significant increasing trend. An increase in SDII over such regions is mainly due to the higher decrease in WD than in PRCPTOT (Figure 9b). On the other hand, the reason for the increase in SDII over the western region is due to an increase in PRCPTOT but decrease in WD. Rising trends in R95, RX1day and RX5day over the WM region further indicate rising high-intensity precipitation extremes over the region. In contrast, decreasing trends in PRCPTOT, R95 and RX1day over the EM and CM region somewhat reinforce a decreasing trend of high-intensity precipitation extremes. Additionally, significant decreasing trends in WD, R10 and R20 indices over EL and CL regions indicate a decrease in the moderate daily precipitation events.

6. Conclusions

First, we have analyzed the spatial distribution of the seasonal precipitation and of a few physically relevant extreme precipitation indices from 210 stations across Nepal over the most recent period, 1981–2010. Then, the spatio-temporal variation of the computed daily precipitation extremes has been analyzed from long-term continuous records available from 76 stations over the period of 1970–2012 using a robust non-parametric Mann−Kendall [33,34] trend test and the trend-free pre-whitening (TFPW) procedure. Trends at local stations are further assessed for their field significance over the seven distinct physio-geographic regions of Nepal, in order to identify the most dominant patterns of changes in extreme precipitation indices over these regions.

By including more stations with updated records and employing robust test statistics as compared to previous studies, this study provides a detailed and coherent picture of spatio-temporal changes in the precipitation means and extremes across the whole of Nepal as well as over its seven physio-geographic sub-regions. Generally, we have found a prolongation of dry periods and a decrease in post-monsoon precipitation across the whole country, while annual and high-intensity precipitation extremes show contrasting evidence of increase in the western half and a moderately decreasing pattern in the east. Similarly, winter precipitation has significantly decreased across the western region, thereby indicating the weakened influence of western disturbances. Such information is anticipated to be useful in decision-making for the effective management of water resources, hydro-meteorologically induced disasters and agricultural practices, health and other climate-related livelihood activities in different regions as well as for the verification of climate model projections across Nepal. Similarly, the presented picture can support in strengthening the weather, climate and flood early warning and forecasting systems, in devising the landslide, flood risk and vulnerability maps, in adapting to region-specific drought-tolerant crops and in designing reservoir-type multipurpose hydropower projects. However, we caution that the presented findings should preferably be interpreted in connection with other relevant factors, such as population density, agricultural yield, food deficit regions, poverty, and the areas which have least access to post-disaster relief facilities and low coping capacity. Further, the shortcoming of the presented analysis is mainly the lack of high-altitude stations and thus the results may not be representative for the high mountainous regions, such as the western high mountains (WH) and eastern high mountains (EH). Hence, future research should focus on employing a broader database and larger set of extreme indices for the comprehensive analysis of changes in precipitation extremes at the seasonal scale in order to understand the physical mechanisms driving such changes. The main findings of the study are summarized below:

- Spatial distribution of monsoonal precipitation across Nepal indicates three high-precipitation pocket areas, such as surrounding regions of Lumle, Gumthang and Num, and four regions of low precipitation on the leeward side of high mountains, namely, Mustang, Manang, Dolpa, and Everest. Likewise, depending on the orientation of surrounding mountain ranges, lower precipitation is also found in the river valleys lying within the middle mountains and hill regions. Pre- and post-monsoonal precipitation more or less follow the spatial pattern of monsoonal precipitation in terms of representing three-peak precipitation pocket areas, as well as the east to west gradient. In contrast to other seasons, winter precipitation is higher over the western middle and high mountainous (WM) areas and lower over the eastern lowlands (EL), clearly depicting west to east and north to south gradients.
- Spatial distribution of precipitation extremes suggests that the high-intensity-related extremes (95th and 99th percentile thresholds and one-day extreme precipitation) are relatively more intense over the southern lowlands as compared to other regions suggesting higher chances of flooding and inundation in the region. However, the frequency-related extreme indices (WD—wet days, R10 and R20—heavy and very heavy precipitation days) generally feature low values.
- Long-term trends in the monsoonal and annual precipitation (PRCPTOT) indicate their significant increases over the middle mountains and hills within the western region (WM), and over the high mountains within the central region (CH). However, the monsoonal and annual precipitations feature significantly decreasing trends over the whole central and eastern regions, except for the former over the eastern middle-mountain and hills (EM).
- Pre-monsoon precipitation features a significant positive trend over the central high mountain region (CH) and over all lowland regions. On the other hand, winter precipitation features a decreasing trend over most of Nepal; however, such a trend is significant only over the western middle mountains and hills (WM). Similarly, a significantly decreasing trend in the post-monsoonal precipitation has also been observed across Nepal, except over CH and WL.
- A coherent significant positive trend in the high-intensity-related extreme precipitation indices (RX1day, RX5day and R95) has been observed over the middle mountains and hills of the western region (WM) and central high mountains (CH), suggesting more intense precipitation therein. This is further supported by the evidence of significant positive trends in the monsoonal and annual precipitation, with a negative trend in the wet days over that region. In contrast, decreasing trends in the annual precipitation, wet days (WD) and high-intensity-related precipitation extremes (R95, RX1day), together with an increasing trend in the consecutive dry days (CDD) over the central and eastern middle mountains and hills reveals weakening of the intense precipitation extremes.
- Significant positive trend in consecutive dry days (CDD) but negative trend in wet days (WD) are observed across the country, suggesting the prolongation of the dry period.

Supplementary Materials: The following are available online at www.mdpi.com/2225-1154/5/1/04/s1, this manuscript includes Table S1: Stationwise significance of extreme indices and field significance.

Acknowledgments: The authors would like to thank the Department of Hydrology and Meteorology, Nepal, for the permission to use meteorological data. Ramchandra Karki's PhD scholarship was supported by Deutscher Akademischer Austauschdienst (DAAD) under the Research Grants—Doctoral Programmes in Germany, through University of Hamburg, Germany. Further, we acknowledge the TREELINE project funded by the German Research Foundation (SCHI 436/14-1, BO 1333/4-1, SCHO 739/14-1). Finally, we would like to thank the three anonymous reviewers for their valuable comments and suggestions which helped us on improving this paper.

Author Contributions: Ramchandra Karki initiated, designed the study, performed the data analysis and wrote the paper with critical input and contribution on analysis, interpretation of the results and writing from Shabeh ul Hasson and Jürgen Böhner while Udo Schickhoff and Thomas Scholten have contributed to the analysis and interpretation of the results.

Conflicts of Interest: The authors declare no conflict of interest.

References

1. Karl, T.R.; Knight, R.W. Secular trends of precipitation amount, frequency, and intensity in the United States. *Bull. Am. Meteorol. Soc.* **1998**, *79*, 231–241. [CrossRef]
2. Kunkel, K.E.; Easterling, D.R.; Redmond, K.; Hubbard, K. Temporal variations of extreme precipitation events in the United States: 1895–2000. *Geophys. Res. Lett.* **2003**, *30*, 51–54. [CrossRef]
3. Kunkel, K.E.; Easterling, D.R.; Kristovich, D.A.R.; Gleason, B.; Stoecker, L.; Smith, R. Recent increases in U.S. heavy precipitation associated with tropical cyclones. *Geophys. Res. Lett.* **2010**, *37*, 2–5. [CrossRef]
4. Alexander, L.V.; Zhang, X.; Peterson, T.C.; Caesar, J.; Gleason, B.; Klein Tank, A.M.G.; Haylock, M.; Collins, D.; Trewin, B.; Rahimzadeh, F.; et al. Global observed changes in daily climate extremes of temperature and precipitation. *J. Geophys. Res. Atmos.* **2006**, *111*, D05109. [CrossRef]
5. Klein Tank, A.M.G.; Peterson, T.C.; Quadir, D.A.; Dorji, S.; Zou, X.; Tang, H.; Santhosh, K.; Joshi, U.R.; Jaswal, A.K.; Kolli, R.K.; et al. Changes in daily temperature and precipitation extremes in central and south Asia. *J. Geophys. Res.* **2006**, *111*, D16105. [CrossRef]
6. Dai, A. Drought under global warming: A review. *WIREs Clim. Chang.* **2011**, *2*, 45–65. [CrossRef]
7. Coumou, D.; Rahmstorf, S. A decade of weather extremes. *Nat. Clim. Chang.* **2012**, *2*, 491–496. [CrossRef]
8. Groisman, P.Y.; Knight, R.W.; Karl, T.R. Changes in intense precipitation over the central United States. *J. Hydrometeorol.* **2011**, *13*, 47–66. [CrossRef]
9. Stocker, T.F.; Qin, D.; Platner, G.K. *IPCC Climate Change 2013: The Physical Science Basis*; Intergovernmental Panel on Climate Change Working Group I Contribution to the Fifth Assessment Report (AR5); Cambridge University Press: New York, NY, USA, 2013.
10. Westra, S.; Alexander, L.V.; Zwiers, F.W. Global increasing trends in annual maximum daily precipitation. *J. Clim.* **2013**, *26*, 3904–3918. [CrossRef]
11. Sheikh, M.M.; Manzoor, N.; Ashraf, J.; Adnan, M.; Collins, D.; Hameed, S.; Manton, M.J.; Ahmed, A.U.; Baidya, S.K.; Borgaonkar, H.P.; et al. Trends in extreme daily rainfall and temperature indices over South Asia. *Int. J. Climatol.* **2014**, *1637*, 1625–1637. [CrossRef]
12. United Nations Environment Programme (UNEP). *GEO Year Book 2003*; UNEP: Nairobi, Kenya, 2003.
13. Caesar, J.; Alexander, L.V.; Trewin, B.; Tse-ring, K.; Sorany, L.; Vuniyayawa, V.; Keosavang, N.; Shimana, A.; Htay, M.M.; Karmacharya, J.; et al. Changes in temperature and precipitation extremes over the Indo-Pacific region from 1971 to 2005. *Int. J. Climatol.* **2011**, *31*, 791–801. [CrossRef]
14. Donat, M.G.; Alexander, L.V.; Yang, H.; Durre, I.; Vose, R.; Dunn, R.J.H.; Willett, K.M.; Aguilar, E.; Brunet, M.; Caesar, J.; et al. Updated analyses of temperature and precipitation extreme indices since the beginning of the twentieth century: The HadEX2 dataset. *J. Geophys. Res. Atmos.* **2013**, *118*, 2098–2118. [CrossRef]
15. Goswami, B.N.; Venugopal, V.; Sengupta, D.; Madhusoodanan, M.S.; Xavier, P.K. Increasing trend of extreme rain events over India in a warming environment. *Science* **2006**, *314*, 1442–1445. [CrossRef] [PubMed]
16. Joshi, U.R.; Rajeevan, M. *Trends in Precipitation Extremes over India*; Research Report No.: 3/2006; National Climate Centre, India Meteorological Department: Pune, India, 2006.
17. Rajeevan, M.; Bhate, J.; Jaswal, A.K. Analysis of variability and trends of extreme rainfall events over India using 104 years of gridded daily rainfall data. *Geophys. Res. Lett.* **2008**, *35*, L18708.
18. Krishnamurthy, C.K.B.; Lall, U.; Kwon, H.H. Changing frequency and intensity of rainfall extremes over India from 1951 to 2003. *J. Clim.* **2009**, *22*, 4737–4746. [CrossRef]
19. Pattanaik, D.R.; Rajeevan, M. Variability of extreme rainfall events over India during southwest monsoon season. *Meteorol. Appl.* **2010**, *17*, 88–104. [CrossRef]
20. Hussain, M.S.; Lee, S. The regional and the seasonal variability of extreme precipitation trends in Pakistan. *Asia Pac. J. Atmos. Sci.* **2013**, *49*, 421–441. [CrossRef]
21. Roy, S.S.; Balling, R.C. Trends in extreme daily precipitation indices in India. *Int. J. Climatol.* **2004**, *24*, 457–466.
22. Revadekar, J.V.; Hameed, S.; Collins, D.; Manton, M.; Sheikh, M.; Borgaonkar, H.P.; Kothawale, D.R.; Adnan, M.; Ahmed, A.U.; Ashraf, J.; et al. Impact of altitude and latitude on changes in temperature extremes over South Asia during 1971–2000. *Int. J. Climatol.* **2013**, *33*, 199–209. [CrossRef]
23. 2013 North India floods. Available online: https://en.wikipedia.org/wiki/2013_North_India_floods (accessed on 25 October 2014).

24. Nepal: Landslides and Floods Information Bulletin. Available online: http://reliefweb.int/report/nepal/nepal-landslides-and-floods-information-bulletin-n-1-17-august-2014 (accessed on 25 October 2014).
25. Ministry of Agriculture and Cooperatives (MOAAC); World Food Programme (WFP); Food and Agriculture Organization (FAO). *2008/09 Winter Drought in Nepal-Crop and Food Security Assessment Joint Technical Report*; Ministry of Agriculture and Cooperatives, Government of Nepal, World Food Programme, Food and Agriculture Organization of the United Nations: Kathmandu, Nepal, 2009.
26. Revadekar, J.V.; Preethi, B. Statistical analysis of the relationship between summer monsoon precipitation extremes and foodgrain yield over India. *Int. J. Climatol.* **2012**, *32*, 419–429. [CrossRef]
27. Central Bureau of Statistics (CBS). *Statistical Information on Nepalese Agriculture*; Central Bureau of Statistics: Kathmandu, Nepal, 2013.
28. Baidya, S.K.; Shrestha, M.L.; Sheikh, M.M. Trends in daily climatic extremes of temperature and precipitation in Nepal. *J. Hydrol. Meteorol.* **2008**, *5*, 1.
29. Duncan, J.M.A.; Biggs, E.M.; Dash, J.; Atkinson, P.M. Spatio-temporal trends in precipitation and their implications for water resources management in climate-sensitive Nepal. *Appl. Geogr.* **2013**, *43*, 138–146. [CrossRef]
30. Hofstra, N.; Haylock, M.; New, M.; Jones, P.D. Testing E-OBS European high-resolution gridded data set of daily precipitation and surface temperature. *J. Geophys. Res. Atmos.* **2009**. [CrossRef]
31. Sharma, K.P. *Climate Change: Trends and Impacts on the Livelihoods of People*; Technical Report; Jalsrot Vikas Sanstha/Nepal Water Partnership: Kathmandu, Nepal, 2009.
32. Shrestha, A.B.; Bajracharya, S.R.; Sharma, A.R.; Duo, C.; Kulkarni, A. Observed trends and changes in daily temperature and precipitation extremes over the Koshi river basin 1975–2010. *Int. J. Climatol.* **2016**. [CrossRef]
33. Mann, H.B. Nonparametric tests against trend. *Econometrica* **1945**, *13*, 245–259. [CrossRef]
34. Kendall, M.G. *Rank Correlation Method*; Griffin: London, UK, 1975.
35. Kansakar, S.R.; Hannah, D.M.; Gerrard, J.; Rees, G. Spatial pattern in the precipitation regime in Nepal. *Int. J. Climatol.* **2004**, *24*, 1645–1659. [CrossRef]
36. Shrestha, A.B.; Aryal, R. Climate change in Nepal and its impact on Himalayan glaciers. *Reg. Environ. Chang.* **2010**, *11*, 65–77. [CrossRef]
37. Duncan, J.M.A.; Biggs, E.M. Assessing the accuracy and applied use of satellite-derived precipitation estimates over Nepal. *Appl. Geogr.* **2012**, *34*, 626–638. [CrossRef]
38. Karki, R.; Talchabhadel, R.; Aalto, J.; Baidya, S.K. New climatic classification of Nepal. *Theor. Appl. Climatol.* **2016**, *125*, 799–808. [CrossRef]
39. Nayava, J.L. Rainfall in Nepal. *Himal. Rev.* **1981**, *12*, 1–18.
40. Lang, T.J.; Barros, A.P. Winter storms in the central Himalayas. *J. Meteorol. Soc. Jpn.* **2004**, *82*, 829–844. [CrossRef]
41. Böhner, J. General climatic controls and topoclimatic variations in Central and High Asia. *Boreas* **2006**, *35*, 279–295. [CrossRef]
42. Böhner, J.; Miehe, G.; Miehe, S.; Nagy, L. Climate and weather variability: An introduction to the natural history, ecology, and human environment of the Himalayas, a companion volume to the flora of Nepal. *R. Bot. Gard. Edinb.* **2015**, *4*, 23–89.
43. Hasson, S.; Lucarini, V.; Pascale, S. Hydrological cycle over South and Southeast Asian river basins as simulated by PCMDI/CMIP3 experiments. *Earth Syst. Dyn.* **2013**, *4*, 199–217. [CrossRef]
44. Ichiyanagi, K.; Yamanaka, M.D.; Muraji, Y.; Vaidya, V.K. Precipitation in Nepal between 1987 and 1996. *Int. J. Climatol.* **2007**, *27*, 1753–1762. [CrossRef]
45. Barros, A.P.; Kim, G.; Williams, E.; Nesbitt, S.W. Probing orographic controls in the Himalayas during the monsoon using satellite imagery. *Nat. Hazards Earth Syst. Sci.* **2004**, *4*, 29–51. [CrossRef]
46. Dhar, O.N.; Nandargi, S. Areas of heavy precipitation in the Nepalese Himalayas. *Weather* **2005**, *12*, 354–356. [CrossRef]
47. Bookhagen, B.; Burbank, D.W. Topography, relief, and TRMM-derived rainfall variations along the Himalaya. *Geophys. Res. Lett.* **2006**, *33*, L08405.
48. Miehe, G. *Langtang Himal. A Prodormus of the Vegetation Ecology of the Himalayas. Mit Einer Kommentierten Flechtenliste von Josef Poelt*; Borntrager: Stuttgart, Germany, 1990.

49. Putkonen, J. Continuous snow and rain data at 500 to 4400 m altitude near Annapurna, Nepal, 1999–2001. *Arct. Antarct. Alp. Res.* **2004**, *36*, 244–248. [CrossRef]
50. Salerno, F.; Guyennon, N.; Thakuri, S.; Viviano, G.; Romano, E.; Vuillermoz, E.; Cristofanelli, P.; Stocchi, P.; Agrillo, G.; Ma, Y.; et al. Weak precipitation, warm winters and springs impact glaciers of south slopes of Mt. Everest (central Himalaya) in the last 2 decades (1994–2013). *Cryosphere* **2015**, *9*, 1229–1247. [CrossRef]
51. Gerlitz, L.; Bechtel, B.; Böhner, J.; Bobrowski, M.; Bürzle, B.; Müller, M.; Scholten, T.; Schickhoff, U.; Schwab, N.; Weidinger, J. Analytic comparison of temperature lapse rates and precipitation gradients in a Himalayan treeline environment: Implications for statistical downscaling. In *Climate Change, Glacier Response, and Vegetation Dynamics in the Himalaya: Contributions toward Future Earth Initiatives*; Singh, R.B., Schickhoff, U., Mal, S., Eds.; Springer: Cham, Switzerland, 2016; pp. 49–64.
52. Barros, A.P.; Lang, T.J. Monitoring the Monsoon in the Himalayas: Observations in Central Nepal, June 2001. *Mon. Weather Rev.* **2003**, *131*, 1408–1427. [CrossRef]
53. Shrestha, A.B.; Awake, C.P.; Dibb, J.E.; Mayewski, P.A. Precipitation fluctuations in the Nepal Himalaya and its vicinity and relationship with some large scale climatological parameters. *Int. J. Climatol.* **2000**, *2*, 317–327. [CrossRef]
54. Sharma, K.P.; Moore, B., III; Vorosmarty, C.J. Anthropogenic, climatic and hydrologic trends in the Koshi Basin, Himalaya. *Clim. Chang.* **2000**, *47*, 141–165. [CrossRef]
55. Shrestha, M.L. Interannual variation of summer monsoon rainfall over Nepal and its relation to southern oscillation index. *Meteorol. Atmos. Phys.* **2000**, *75*, 21–28. [CrossRef]
56. Gautam, D.K.; Regmi, S.K. Recent trends in the onset and withdrawal of summer monsoon over Nepal. *Ecopersia* **2013**, *1*, 353–367.
57. Panthi, J.; Dahal, P.; Shrestha, M.; Aryal, S.; Krakauer, N.; Pradhanang, S.; Lakhankar, T.; Jha, A.; Sharma, M.; Karki, R. Spatial and temporal variability of rainfall in the Gandaki River Basin of Nepal Himalaya. *Climate* **2015**, *3*, 210–226. [CrossRef]
58. Talchabhadel, R.; Karki, R.; Parajuli, B. Intercomparison of precipitation measured between automatic and manual precipitation gauge in Nepal. *Measurement* **2016**. [CrossRef]
59. Zhang, X.; Yang, F. *User Manual; RClimDex 1.0*; Climate Research Branch Environment: Downsview, ON, Canada, 2004.
60. Vincent, L.A.; Peterson, T.C.; Barros, V.R.; Marino, M.B.; Rusticucci, M.; Carrasco, G.; Ramirez, E.; Alves, L.M.; Ambrizzi, T.; Berlato, M.A.; et al. observed trends in indices of daily temperature extremes in South America 1960–2000. *J. Clim.* **2005**, *18*, 5011–5023. [CrossRef]
61. Aguilar, E.; Auer, I.; Brunet, M.; Peterson, T.C.; Wieringa, J. *Guidelines on Climate Metadata and Homogenization*; World Meteorological Organization: Geneva, Switzerland, 2003.
62. Wang, X.L. Penalized maximal F-test for detecting undocumented mean-shifts without trend-change. *J. Atmos. Ocean. Techol.* **2008**, *25*, 368–384. [CrossRef]
63. Hasson, S.; Böhner, J.; Lucarini, V. Prevailing climatic trends and runoff response from Hindukush–Karakoram–Himalaya, upper Indus basin. *Earth Syst. Dyn.* **2015**, *6*, 579–653. [CrossRef]
64. Hasson, S.U.; Gerlitz, L.; Schickhoff, U.; Scholten, T.; Böhner, J. Recent climate change over High Asia. In *Climate Change, Glacier Response, and Vegetation Dynamics in the Himalaya: Contributions toward Future Earth Initiatives*; Singh, R.B., Schickhoff, U., Mal, S., Eds.; Springer: Cham, Switzerland, 2016; pp. 29–48.
65. Duan, W.; He, B.; Takara, K.; Luo, P.; Hu, M.; Alias, N.E.; Nover, D. Changes of precipitation amounts and extremes over Japan between 1901 and 2012 and their connection to climate indices. *Clim. Dyn.* **2015**, *45*, 2273–2292. [CrossRef]
66. Zhang, X.; Alexander, L.; Hegerl, G.C.; Jones, P.; Tank, A.K.; Peterson, T.C.; Trewin, B.; Zwiers, F.W. Indices for monitoring changes in extremes based on daily temperature and precipitation data. *WIREs Clim. Chang.* **2011**, *2*, 851–870. [CrossRef]
67. Bookhagen, B. Appearance of extreme monsoonal rainfall events and their impact on erosion in the Himalaya. *Geomat. Nat. Hazards Risk* **2010**, *1*, 37–50. [CrossRef]
68. Casanueva, A.; Rodríguez-Puebla, C.; Frías, M.D.; González-Reviriego, N. Variability of extreme precipitation over Europe and its relationships with teleconnection patterns. *Hydrol. Earth Syst. Sci.* **2014**, *18*, 709–725. [CrossRef]
69. Sen, P.K. Estimates of the regression coefficient based on Kendall's tau. *J. Am. Stat. Assoc.* **1968**, *63*, 1379–1389. [CrossRef]

70. Theil, H. A rank-invariant method of linear and polynomial regression analysis, I, II, III. In *Henri Theil's Contributions to Economics and Econometrics*; Springer: Amsterdam, The Netherlands, 1992; pp. 386–392, 512–525, 1397–1412.
71. Douglas, E.M.; Vogel, R.M.; Kroll, C.N. Trends in floods and low flows in the United States: Impact of spatial correlation. *J. Hydrol.* **2000**, *240*, 90–105. [CrossRef]
72. Zhang, X.; Vincent, L.A.; Hogg, W.D.; Niitsoo, A. Temperature and precipitation trends in Canada during the 20th century. *Atmos. Ocean* **2000**, *38*, 395–429. [CrossRef]
73. Yue, S.; Wang, C.Y. Regional streamflow trend detection with consideration of both temporal and spatial correlation. *Int. J. Climatol.* **2002**, *22*, 933–946. [CrossRef]
74. Yue, S.; Pilon, P.; Phinney, B. Canadian streamflow trend detection: Impacts of serial and cross-correlation. *Hydrol. Sci. J.* **2003**, *48*, 51–63. [CrossRef]
75. Yue, S.; Pilon, P.; Phinney, B.; Cavadias, G. The influence of autocorrelation on the ability to detect trend in hydrological series. *Hydrol. Process.* **2002**, *16*, 1807–1829. [CrossRef]
76. Von Storch, V.H. Misuses of statistical analysis in climate research. In *Analysis of Climate Variability: Applications of Statistical Techniques*; von Storch, H., Navarra, A., Eds.; Springer: Berlin, Germany, 1995; pp. 11–26.
77. Hamed, K.H.; Rao, A.R. A modified Mann-Kendall trend test for autocorrelated data. *J. Hydrol.* **1998**, *204*, 182–196. [CrossRef]
78. Burn, D.H.; Cunderlik, J.; Pietroniro, A. Climatic influences on streamflow timing in the headwaters of the Mackenzie River Basin. *J. Hydrol.* **2008**, *352*, 225–238. [CrossRef]
79. Shadmani, M.; Marofi, S.; Roknian, M. Trend analysis in reference evapotranspiration using Mann-Kendall and Spearman's Rho tests in arid regions of Iran. *Water Resour. Manag.* **2012**, *26*, 211–224. [CrossRef]
80. Wu, H.; Soh, L.; Samal, A. Trend analysis of streamflow drought events in Nebraska. *Water Resour. Manag.* **2008**, *22*, 145–164. [CrossRef]
81. Lacombe, G.; McCartney, M. Uncovering consistencies in Indian rainfall trends observed over the last half century. *Clim. Chang.* **2014**, *123*, 287–299. [CrossRef]
82. Vogel, R.M.; Kroll, C.N. Low-flow frequency analysis using probability plot correlation coefficients. *J. Water Resour. Plan. Manag.* **1989**, *115*, 338–357. [CrossRef]
83. Lettenmaier, D.P.; Wood, E.F.; Wallis, J.R. Hydro-climatological trends in the continental United-States, 1948–88. *J. Clim.* **1994**, *7*, 586–607. [CrossRef]
84. Livezey, R.E.; Chen, W.Y. Statistical field significance and its determination by Monte Carlo techniques. *Mon. Weather Rev.* **1983**, *111*, 46–59. [CrossRef]
85. Ventura, V.; Paciorek, C.J.; Risbey, J.S. Controlling the proportion of falsely rejected hypotheses when conducting multiple tests with climatological data. *J. Clim.* **2004**, *17*, 4343–4356. [CrossRef]
86. Renard, B.; Lang, M. Use of a Gaussian copula for multivariate extreme value analysis: Some case studies in hydrology. *Adv. Water Resour.* **2007**, *30*, 897–912. [CrossRef]
87. Efron, B. Bootstrap methods: Another look at the Jackknife. *Ann. Stat.* **1979**, *7*, 1–26. [CrossRef]
88. Weibull, W. A statistical theory of strength of materials. *Ing. Vetensk. Akad. Handl.* **1939**, *151*, 1–45.
89. Petrow, T.; Merz, B. Trends in flood magnitude, frequency and seasonality in Germany in the period 1951–2002. *J. Hydrol.* **2009**, *371*, 129–141. [CrossRef]
90. Department of Hydrology and Meteorology (DHM). *Study of Climate and Climatic Variation over Nepal*; Technical Report; Department of Hydrology and Meteorology: Kathmandu, Nepal, 2015. Available online: http://www.dhm.gov.np/climate/ (accessed on 1 October 2016).
91. Shrestha, D.; Singh, P.; Nakamura, K. Spatiotemporal variation of rainfall over the central Himalayan region revealed by TRMM precipitation radar. *J. Geophys. Res. Atmos.* **2012**, *117*, D22106. [CrossRef]
92. Dahal, R.K.; Hasegawa, S. Representative rainfall thresholds for landslides in the Nepal Himalaya. *Geomorphology* **2008**, *100*, 429–443. [CrossRef]
93. Practical Action Nepal Office. *Temporal and Spatial Variability of Climate Change over Nepal (1976–2005)*; Technical Report; Practical Action Nepal Office: Kathmandu, Nepal, 2009; Available online: http://practicalaction.org/file/region_nepal/ClimateChange1976--2005.pdf (accessed on 4 October 2014).
94. Mäkelä, A.; Shrestha, R.; Karki, R. Thunderstorm characteristics in Nepal during the pre-monsoon season 2012. *Atmos. Res.* **2014**, *137*, 91–99. [CrossRef]

95. Hasson, S.U.; Pascale, S.; Lucarini, V.; Böhner, J. Seasonal cycle of precipitation over major river basins in South and Southeast Asia: A review of the CMIP5 climate models data for present climate and future climate projections. *Atmos. Res.* **2016**, *180*, 42–63. [CrossRef]
96. Hasson, S.; Lucarini, V.; Pascale, S.; Böhner, J. Seasonality of the hydrological cycle in major South and Southeast Asian river basins as simulated by PCMDI/CMIP3 experiments. *Earth Syst. Dyn.* **2014**, *5*, 67–87. [CrossRef]
97. Nayava, J.L. Variations of rice yield with rainfall in Nepal during 1971–2000. *J. Hydrol. Meteorol.* **2008**, *5*, 93–102.
98. Khatiwada, K.R.; Panthi, J.; Shrestha, M.L. Hydro-climatic variability in the Karnali River Basin. *Climate* **2016**. [CrossRef]
99. Dahal, P.; Shrestha, N.S.; Shrestha, M.L.; Krakauer, N.Y.; Panthi, J.; Pradhanang, S.M.; Jha, A.; Lakhankar, T. Drought risk assessment in central Nepal: Temporal and spatial analysis. *Nat. Hazards* **2016**, *80*, 1913–1932. [CrossRef]
100. Aryal, S. Rainfall and water requirement of rice during growing period. *J. Agric. Environ.* **2012**, *13*, 1–4. [CrossRef]
101. Wang, S.Y.; Yoon, J.H.; Gillies, R.R.; Cho, C. What caused the winter drought in western Nepal during recent years? *J. Clim.* **2013**, *26*, 8241–8256. [CrossRef]
102. Cannon, F.; Carvalho, L.M.V.; Jones, C.; Bookhagen, B. Multi-annual variations in winter westerly disturbance activity affecting the Himalaya. *Clim. Dyn.* **2015**, *44*, 441–455. [CrossRef]
103. Shekhar, M.S.; Chand, H.; Kumar, S.; Srinivasan, K.; Ganju, A. Climate-change studies in the western Himalaya. *Ann. Glaciol.* **2010**, *51*, 105–112. [CrossRef]
104. Sigdel, M.; Ma, Y. Variability and trends in daily precipitation extremes on the northern and southern slopes of the central Himalaya. *Theor. Appl. Climatol.* **2016**. [CrossRef]
105. Cho, C.; Li, R.; Wang, S.Y.; Ho, J.; Robert, Y. Anthropogenic footprint of climate change in the June 2013 Northern India flood. *Clim. Dyn.* **2016**, *46*, 797–805. [CrossRef]
106. Vellore, R.K.; Kaplan, M.L.; Krishnan, R.; Lewis, J.M.; Sabade, S.; Deshpande, N.; Singh, B.B.; Madhura, R.K.; Rama Rao, M.V.S. Monsoon-extratropical circulation interactions in Himalayan extreme rainfall. *Clim. Dyn.* **2016**, *46*, 3517–3546. [CrossRef]
107. Vellore, R.K.; Krishnan, R.; Pendharkar, J.; Choudhury, A.D.; Sabin, T.P. On the anomalous precipitation enhancement over the Himalayan foothills during monsoon breaks. *Clim. Dyn.* **2014**, *43*, 2009–2031. [CrossRef]
108. Song, X.; Song, S.; Sun, W.; Mu, X.; Wang, S.; Li, J.; Li, Y. Recent changes in extreme precipitation and drought over the Songhua River Basin, China, during 1960–2013. *Atmos. Res.* **2015**, *157*, 137–152. [CrossRef]
109. Shahid, S. Trends in extreme rainfall events of Bangladesh. *Theor. Appl. Climatol.* **2011**, *104*, 489–499. [CrossRef]
110. Sigdel, M.; Ikeda, M. Spatial and temporal analysis of drought in Nepal using standardized precipitation index and its relationship with climate indices. *J. Hydrol. Meteorol.* **2010**, *7*, 59–74. [CrossRef]
111. Kafle, H.K. Spatial and temporal variation of drought in far and mid-western regions of Nepal: Time series analysis (1982–2012). *Nepal J. Sci. Technol.* **2014**, *15*, 65–76. [CrossRef]
112. Miyan, M.A. Droughts in Asian least developed countries: Vulnerability and sustainability. *Weather Clim. Extremes* **2015**, *7*, 8–23. [CrossRef]
113. Yao, T.; Thompson, L.; Yang, W.; Yu, W.; Gao, Y.; Guo, X.; Yang, X.; Duan, K.; Zhao, H.; Xu, B.; et al. Different glacier status with atmospheric circulations in Tibetan Plateau and surroundings. *Nat. Clim. Chang.* **2012**, *2*, 663–667. [CrossRef]
114. Manton, M.J.; Haylock, M.R.; Hennessy, K.J.; Nicholls, N.; Chambers, L.E.; Collins, D.A.; Daw, G.; Finet, A.; Gunawan, D.; Inape, K.; et al. Trends in extreme daily rainfall and temperature in Southeast Asia and the South Pacific: 1961–1998. *Int. J. Climatol.* **2001**, *21*, 269–284. [CrossRef]